Vokasi Unesa Bulletin of Engineering, Technology and Applied Science (VUBETA)
https://journal.unesa.ac.id/index.php/vubeta
Vol. 2, No. 3, 2025, pp. 387~400 DOI: 10.26740/vubeta.v2i3.39269
ISSN: 3064-0768

A Novel Modified Tornado optimizer with Coriolis Force Based on Levy Flight to Optimize Parameters Proportional Integral Derivative of DC Motor

Diego Oliva[1*], Widi Aribowo[2], Farhad Soleimanian Gharehchopogh[3], Vugar Hacimahmud Abdullayev[4], Asmunin[5], Andi Iwan Nurhidayat[5]

[1]Departamento de Ingeniería Electro-Fotónica, Universidad de Guadalajara, Guadalajara, México
[2]Department of Electrical Engineering, Faculty of Vocational Studies, Universitas Negeri Surabaya, Surabaya, Indonesia, Indonesia
[3]Department of Computer Engineering, Urmia Branch, Islamic Azad University, Urmia, Iran
[4]Department of Computer Engineering, Azerbaijan State Oil and Industry University, Baku, Azerbaijan
[5]Informatics Management Study Program, Faculty of Vocational Studies, Universitas Negeri Surabaya, Surabaya, Indonesia

Article Info

Article history:

Received March 12, 2025
Revised April 19, 2025
Accepted June 20, 2025

Keywords:

DC Motor
Metaheuristic
Levy Flight
Tornado Optimizer
Artificial Intelligence

ABSTRACT

One kind of electric motor that runs on direct current (DC) is called a DC (Direct Current) motor. This motor uses the interaction of electric current and magnetic fields to transform electrical energy into mechanical energy, or motion. Applications requiring exact speed and torque control frequently use DC motors. By minimizing errors (differences between setpoints and actual values), proportional-integral-derivative (PID) control is a control technique used to govern dynamic systems to reach desired conditions (setpoints). PID creates an ideal control signal by combining three elements. The Modified Tornado optimizer-based Coriolis force (TOC) method for DC motor control is presented in this article. The paradigm for the TOC approach is the Tornado Optimizer-Based Coriolis Force Algorithm, a metaheuristic that leverages tornado dynamics and the effect of the Coriolis force to address difficult optimization problems. According to this study, the TOC method can be improved by implementing the Levy Flight methodology. According to the results of tests employing optimal functions, the LTOC technique may broaden exploration and exploitation. Meanwhile, when the LTOC technique is applied as a DC motor controller, the optimal overshoot response value is achieved. The LTOC approach outperforms the TOC method by 0.014% and 0.037%, respectively, in terms of ITSE and ITAE values.

1. INTRODUCTION

Electrical energy efficiency is the ability of a device, system, or process to use electrical energy optimally while minimizing waste [1]-[3]. Energy efficiency means getting the maximum result (output) from the electrical energy used (input). The higher the energy efficiency, the less energy is wasted in heat or other forms. By implementing the principles of electrical energy efficiency, we save money and contribute to environmental preservation and future energy sustainability [4]-[6]. DC motors are one type of electric motor that is very important in various applications because of their ability to be controlled precisely. Despite some disadvantages, such as higher maintenance requirements and costs, DC motors remain the primary choice in many industrial, household, and transportation applications [7]-[9]. With the advancement of technology, DC motors continue to evolve. DC motors are used in various applications because of their flexibility and controllability [10]-[13]. Some examples of DC motor applications are: Use in automated devices such as automatic garage doors, Production machinery that requires precise speed and torque control, Electric vehicles such as golf carts, electric bicycles, and electric trains, and used in robots to drive robotic arms or wheels [14]-[17].

*Corresponding Author
Email: diego.oliva@cucei.udg.mx

PID controllers are very popular because of their ability to provide fast, accurate, and stable responses to changing system conditions [18][19]. This control is widely used in various fields, including industry, robotics, automotive, and electronics. PID control is a potent and flexible tool for managing dynamic systems [20]-[22]. PID controllers can provide fast, accurate, and stable responses by combining proportional, integral, and derivative components. Despite some limitations, PID remains the primary choice in many modern industrial and technological applications [23][24].

The development of AI has changed the world in unprecedented ways [25]-[28]. From simple applications like chatbots to advanced technologies like autonomous vehicles and generative AI, AI continues to advance incredibly [29]-[32]. However, to ensure AI is used responsibly, we must address the challenges of ethics, privacy, and social impact [33]-[36]. With the continued development of supporting technologies such as big data, cloud computing, and quantum computing, AI will continue to open new opportunities and shape a more innovative, more efficient, and more inclusive future.

The development of Proportional-integral-derived (PID) control with the integration of artificial intelligence (AI) has become an essential trend in modern control systems. This combination significantly improves performance, flexibility, and adaptability to complex dynamic conditions. The integration of Artificial Intelligence (AI) into PID Control has opened new opportunities to improve the performance, flexibility, and adaptability of control systems. This technology allows systems to handle complex dynamics, uncertainties, and real-time changes in operating conditions. Despite some challenges in implementation, this development shows excellent potential for revolution in various fields such as industry, robotics, renewable energy, and automotive. Several studies have been presented on the integration of PID with AI, such as reinforcement learning [37], GEO algorithm [38], beetle optimization algorithm [39], cooperation search algorithm [40], Symbiotic Organisms Search Algorithm [41], hybrid butterfly particle swarm optimization [42], gazelle optimizer [43], slap swarm algorithm [44], Fuzzy [45], and Archimedes Optimization Algorithm [46]. Although some researchers have developed PID approaches with AI. But PID parameter optimization with AI can still be explored further to get the best optimization value.

This paper introduces a new optimization method, the Levy Tornado optimizer with Coriolis force (LTOC), which is used for PID parameter estimation in the context of DC motor control. The basic concept and principle of LTOC is from the Tornado optimizer with Coriolis force (TOC), inspired by nature, based on the observation of the tornado cycle process and how thunderstorms and hurricanes evolve into tornadoes using the Coriolis force [47]. The Coriolis force is applied to the windstorm which directly evolves to form a tornado. The contributions of this study are:

a) Improvement of the TOC method by modifying it to combine it with the Levy flight method
b) Application of the LTOC method to DC motors.
c) Validation of the performance of LTOC with TOC using benchmark functions and DC motor performance.

The second section of this paper discusses the DC motor and LTOC approach. Results and discussion make up the third section. Conclusions are drawn in the final section.

2. METHOD

2.1. Tornado optimizer-based Coriolis force

The tornado optimizer with Coriolis force (TOC) posits the existence of numerous windstorms, certain thunderstorms, and precipitation events, wherein windstorms and thunderstorms produce tornadoes, and thunderstorms arise from windstorms. The subsequent section presents the comprehensive mathematical models of the suggested TOC optimizer. The proposed TOC optimizer is a population-based algorithm; thus, the initial stage in the optimization process involves the random generation of a preliminary population of design variables (i.e., windstorms and thunderstorms) between specified upper (u) and lower (l) bounds.

The optimal individuals (i.e., windstorms and thunderstorms), evaluated based on a minimal cost function or, in certain instances, maximal fitness, are chosen to constitute tornadoes, or a singular tornado if only one exists. A selection of effective individuals (i.e., cost function values around the optimal solution) is designated as thunderstorms. In contrast, all other individuals are referred to as windstorms, which ultimately transform into thunderstorms and tornadoes. The initial stage in initiating TOC as an optimization algorithm involves the creation of a population matrix of n persons (i.e., population size) within a d-dimensional search space (i.e., problem dimension). In this context, the location of each windstorm, thunderstorm, and tornado signifies a potential solution to the optimization problem. Equation 21 delineates the method for generating the initial population of windstorms, thunderstorms, and tornadoes inside the search domain using a uniform random initialization process.

$$X_{i,j} = I_j + rand \times (u_j - I_j) \tag{1}$$

$$n_{to} = n_t + n_o \tag{2}$$

$$n_w = n - n_{to} \tag{3}$$

$$y = [y_w, y_t, y_o]_{nxd} = \begin{bmatrix} y_{1,1} & y_{1,d} & y_{1,m} \\ y_{i,1} & y_{i,d} & y_{i,m} \\ y_{N,1} & y_{N,d} & y_{N,m} \end{bmatrix}_{N.d} \tag{4}$$

$$y_w = [y_{w1}, y_{w2}, \ldots\ldots y_{wi}, \ldots y_{wn}] \tag{5}$$

$$y_t = [y_{t1}, y_{t2}, \ldots\ldots y_{ti}, \ldots y_{tn}] \tag{6}$$

$$y_o = [y_{o1}, y_{o2}, \ldots\ldots y_{oi}, \ldots y_{on}] \tag{7}$$

Where $X_{i,j}$ represents the starting value of the ith individual in the jth dimension. $rand$ is a randomly generated number, and $I_{i,j}$ is another randomly generated number. n_t denotes the quantity of thunderstorms, whereas n_o signifies the number of tornadoes, which is established as one in this study. n_w represents the quantity of windstorms, whereas n it signifies the overall population size. $y_{i,j}$ represents the ith candidate individual at dimension j, which may be a windstorm, a thunderstorm, or a tornado. d represents the quantity of design variables (i.e., problem dimension), while the components y_w, y_t, and y_o signify the populations of tornadoes, thunderstorms, and windstorms, respectively. y_{w1} denotes the ith windstorm, y_{t1} signifies the ith thunderstorm, andy_{o1} the ith tornado.

Fitness evaluation

The fitnes value cost (i.e., cos) is calculated for each windstorm and thunderstorm by assessing the cost value as demonstrated below:

$$fit_i = fit(y_i, 1, y_i, 2, y_i, 3, \cdots, y_i, d) \tag{8}$$

$$\overrightarrow{fit} = \begin{bmatrix} fit_i \\ \vdots \\ fit_i \\ \vdots \\ fit_i \end{bmatrix}_{n\times 1} = \begin{bmatrix} fit(y_i) \\ \vdots \\ fit(y_i) \\ \vdots \\ fit(y_n) \end{bmatrix}_{n\times 1} \tag{9}$$

where fit_i denotes the cost value of the i-th individual. where $\overrightarrow{fit}$ is a vector of the obtained fitness functions, and fit_i denotes the value of obtaining the fitness function based on the i-th individual. The fitness function value measures the quality of candidate solutions in meta-heuristic algorithms such as TOC. The population member that produces the best evaluation value for the fitness function is called the best population member. This population member is updated in each round of the proposed optimizer iteration as the candidate solutions are updated. In the proposed optimizer simulation, individuals remain at their locations if they are better than the new location.

Evolution of windstorms

Windstorms typically progress towards tornadoes and thunderstorms, influenced by their volume and intensity of development. This indicates that windstorms develop into tornadoes more frequently than thunderstorms.

$$y_w = \left[y_{w_1}\, y_{w_2} \cdots y_{w_i} \cdots y_{w_{n_w}}\right] = \begin{bmatrix} y_{w_{1,1}} & y_{w_{1,2}} \cdots & y_{w_{1,d}} \\ y_{w_{2,1}} & y_{w_{2,2}} \cdots & y_{w_{2,d}} \\ \vdots & \vdots \quad \vdots & \vdots \\ y_{w_{n_w,1}} & y_{w_{n_w,2}} \cdots & y_{w_{n_w,d}} \end{bmatrix}_{n_w \times d} \tag{9}$$

$$f_k = fit_k - fit_{n_{to}} + 1 \tag{10}$$

$$n_{w_k} = \left\lfloor \left\{ \left| \frac{f_k}{\sum_{k=1}^{n_{to}} f_k} \right| \times n_w \right\} \right\rfloor \tag{11}$$

Where k = 1, 2, 3, … ,n_{to}, and f_k denotes the cost value of the kth thunderstorm associated with a tornado. $n_{w_k}$is the number of tornadoes that evolved or were assigned to a particular thunderstorm or tornado.

Windstorm velocity influenced by the Coriolis effect

Along with extensive atmospheric turbulence, which does not necessitate tornadoes to travel along a linear path, a triadic equilibrium exists between the Coriolis force, the centrifugal force, and the pressure gradient force. The tornado velocity gradient responsible for the formation of thunderstorms and tornadoes can be recognized.

$$\overrightarrow{v_i^{t+1}} = \begin{cases} \eta\left(\mu\overrightarrow{v_i^t} - c\frac{(f\times R_l}{2} + \sqrt{CF_l}\right) & rand \geq 0.5 \\ \eta\left(\mu\overrightarrow{v_i^t} - c\frac{(f\times R_l}{2} + \sqrt{CF_l}\right) & rand \leq 0.5 \end{cases} \quad (12)$$

Where *i*= 1, 2, 3, . . . ,n_w, is the tornado index for a population of size n_w, $\overrightarrow{v_i^{t+1}}$ states the new velocity vector of the tornado to-*i*, $\overrightarrow{v_i^t}$ defines the current velocity vector of the tornado to-*i*, rand refers to random numbers generated with a uniform distribution in the scope [0, 1], η refers to random numbers generated with a uniform distribution in the scope

$$\eta = \frac{2}{\left|2-x-\sqrt{x^2-4x}\right|} \quad (13)$$

Where χ identify the tornado acceleration rate

$$\mu = 0.5 + \frac{rand}{2} \quad (14)$$

$$\mu = 0.5 + \frac{rand}{2} \quad (15)$$

$$R_l = \frac{2}{1+e^{(-t+\frac{T}{2})/2}} \quad (16)$$

$$R_l = \frac{-2}{1+e^{(-t+\frac{T}{2})/2}} \quad (17)$$

Where *rand* represents random numbers generated with a uniform distribution over the range [0, 1]. Where t and T are the current iteration index and the maximum number of iterations.

$$c = b_r \times \delta_1 \times w_r \quad (18)$$

$$\delta_1 = f_d[2 \times rand \quad (19)$$

$$w_r = \frac{2\times rand-(rand+ran\ )}{w_{min}+ran\ \times(w_{maks}-w_{min})} \quad (20)$$

$$f = 2.\Omega \times \sin(-1 + 2 \cdot rand) \quad (21)$$

$$CF_l = \frac{(f^2\times R_l^2)}{4} - R_l \times \phi_i^t \quad (22)$$

$$CF_l = \frac{(f^2\times R_r^2)}{4} - R_r \times \phi_i^t \quad (23)$$

$$\phi_i^t = y_{o_\zeta}^t - y_{w_i}^t \quad (24)$$

re b_r is a constant equal to 100000. f_d represents the value function 1, and -1 represents a change of sign. *rand* is an abbreviation for random values generated in a range [0, 1]. w_{min} dan w_{maks} is a fixed value of each 1,0 and 4,0. Ω is an abbreviation for the angular rate of rotation equal to,7292115E-04 radian s^{-1} rand is a random number generated with a uniform distribution in the range [0, 1]. ϕ_i^t is a component of the pressure gradient force (PGF) which is normal to the current direction of the *i*-th tornado at the *t*-th iteration

$$\zeta = \lceil n_o \times rand(1, n_o) \rceil \quad (25)$$

$$\phi_i^t = \begin{cases} -\phi_i^t \; sgn(R_i) \geq 0 \, , sign(-\phi_i^t) \geq 0 \\ -\phi_i^t \; sgn(R_r) \leq 0 \, , sign(-\phi_i^t) \leq 0 \\ \phi_i^t \; otherwise \end{cases} \tag{26}$$

$$CF_i^t = \begin{cases} - \, CF_i^t \; sgn(\, CF_i^t) < 0 . rnad \geq 0.5 \\ CF_i^t otherwise \end{cases} \tag{27}$$

$$CF_r^t = \begin{cases} - \, CF_r^t \; sgn(\, CF_r^t) < 0 . rnad \geq 0.5 \\ CF_r^t otherwise \end{cases} \tag{28}$$

Where $rand(1, n_o)$ implements a uniformly generated random value vector with a uni-form distribution in the interval [0, 1].

$$\overrightarrow{y_{w_i}^{t+1}} = \overrightarrow{y_{w_i}^t} + 2 \times \alpha \times \left(\overrightarrow{y_{o_i}^t} - rand_w \right) + \overrightarrow{v_i^{t+1}} \tag{29}$$

$$rand_w = \overrightarrow{y_{w_i}}(\lfloor n_w \times rand(1, n_w) \rfloor + 1) \tag{30}$$

$$\alpha = \left| 2a_y \cdot rand - rand \right| \tag{31}$$

$$a_y = \frac{(T - (t^{a_0}/T))}{T} \tag{32}$$

Where $\overrightarrow{y_{w_i}^{t+1}}$dan $\overrightarrow{y_{w_i}^t}$ defines the next and current position vectors of the *i*-th tornado at the *i*-th iteration (t+ 1) dan *t*, each, $\overrightarrow{y_{o_i}^t}$ defines the current position vector of the *i*-th tornado at iteration *t*, $\left(\overrightarrow{y_{o_i}^t} - rand_w \right)$ shows the difference between the evolution of a tornado into a tornado and the random formation of wind, $rand_w$ dan α is a random value. $rand_w$ is the index vector for a randomly selected tornado. a_y represents the exponential parameter. a_0 shows constant value 2,0 and found after extensive analysis.

$$\gamma \epsilon (0, \rho \times x), \rho > 0.5 \tag{33}$$

$$\overrightarrow{y_{w_{J+\sum_1^{n_w} k}}^{t+1}} = \overrightarrow{y_{w_{J+\sum_1^{n_w} k}}^t} + 2 \times rand \times \left(\overrightarrow{y_{t_i}^t} - \overrightarrow{y_{w_{J+\sum_1^{n_w} k}}^t} \right) + 2 \times rand \times \left(\overrightarrow{y_{t_i}^t} - \overrightarrow{y_{w_{J+\sum_1^{n_w} k}}^t} \right) \tag{34}$$

Where *x* is the current distance between the tornado and the thunderstorm, $0.5 < \rho < 2$ where 2 is probably the optimal value of ρ, and γ according to random numbers between 0 and $\rho \times x$ which is uniformly distributed or selected from a reasonable distribution. $\overrightarrow{y_{w_{J+\sum_1^{n_w} k}}^{t+1}}$ dan $\overrightarrow{y_{w_{J+\sum_1^{n_w} k}}^t}$ represents the next and current position vectors of a tornado developing into a thunderstorm at iteration (*t*+ 1) and *t*, respectively, $\overrightarrow{y_{t_i}^t}$ represents the current position vector of the *i*-th thunderstorm at the *t*-th iteration, and $rand$ is a random number generated between 0 and 1 with uniform distribution.

Evolution of a thunderstorm into a tornado

During the research and exploitation phase of the planned optimizer, the new location of the Thunderstorm evolving into a tornado.

$$\overrightarrow{y_{t_i}^t} = \overrightarrow{y_{t_i}^t} + 2 \times \alpha \times \left(\overrightarrow{y_{t_i}^t} - \overrightarrow{y_{o_\zeta}^t} \right) + 2 \times \alpha \times \left(\overrightarrow{y_{t_{\vec{p}}}^t} - \overrightarrow{y_{t_i}^t} \right) \tag{35}$$

$$\vec{p} = \lfloor n_t \cdot rand(1, n_t) + 1 \rfloor \tag{36}$$

Where $\overrightarrow{y_{t_i}^{t+1}}$ dan $\overrightarrow{y_{t_i}^t}$ represents the next and current position vectors of the development of a thunderstorm into a tornado at an iteration (*t*+ 1) and *t*, respectively, $\overrightarrow{y_{o_\zeta}^t}$ identify position vectors for tornadoes at random indices ζ, dan $\overrightarrow{y_{t_{\vec{p}}}^t}$ identify position vectors for thunderstorms.

Random formation of tornadoes

To enhance its exploration capabilities, the suggested TOC-based optimization defines a stochastic tornado formation mechanism. More specifically, TOC is able to avoid immature convergence and local solutions due

to the random tornado creation. In essence, tornadoes develop at random places as they transform into thunderstorms or into tornadoes, producing mature tornadoes at various locations. In order for this process to take place, tornadoes and thunderstorms must be inspected to determine whether they are sufficiently close to the tornado.

$$\overrightarrow{y_{w_i}^{t+1}} = \overrightarrow{y_{w_i}^{t}} - \left(2 \times a_y \times (rand \times (l-u) - l)\right) \times \delta_2$$

$$\left\| \overrightarrow{y_{w_i}^{t}} - \overrightarrow{y_{o_i}^{t}} \right\| < v \tag{37}$$

$$\delta_2 = f_d \lfloor 2 \times rand + 1 \rfloor \tag{38}$$

$$v = \left(0.1 e^{\left(-0.1(t/T)^{0.1}\right)}\right)^{16} \tag{39}$$

$$\overrightarrow{y_{w_{J+\sum_{i=1}^{n_w} k}}^{t+1}} = \overrightarrow{y_{w_{J+\sum_{i=1}^{n_w} k}}^{t}} - \left(2 \times a_y \times (rand \times (l-u) - l)\right) \times \delta_2$$

$$\left\| \overrightarrow{y_{w_i}^{t}} - \overrightarrow{y_{t_i}^{t}} \right\| < v \tag{40}$$

Where *l* and *u* refer to the lower and upper bounds of the search area, respectively. *rand* is a random number that is systematically inserted into the range [0, 1]. δ_2 is the change in sign defined as given in Eq. 38 $\|\cdot\|$ refers to the norm operator, and is an exponential function defined as shown in Eq.. 39, capable of producing small numbers. f_d is a function of the values 1 and -1 to represent a change in sign. *t* represents the current iteration index. *T* represents the maximum iteration index.

2.2. Lévy Flight Optimization

The step length in Levy Flight is determined by a heavy-tailed probability distribution, like the Levy or Pareto distributions. In other words, there is a slight chance of taking a really long stride, but most steps are short. In addition to numerous other uses, this model is frequently used to simulate mathematical optimization, animal behavior, and natural events.

$$L(X_j) \approx \left|X_j\right|^{1-\alpha} \tag{41}$$

$$f_L(x;\alpha,\gamma) = \frac{1}{\pi}\int_0^{\infty} exp(-\gamma q^{\alpha}) \cos\ (qx)\ dq \tag{42}$$

$$f_L(x;\alpha,\gamma) = \frac{\gamma \Gamma(1+\alpha)\sin(\frac{\alpha\pi}{2})}{\pi X^{(1+\alpha)}}, x\ \to \infty \tag{43}$$

$$Levy(\alpha) = 0.05 \times \frac{x}{|y|^{1/\alpha}} \tag{44}$$

$$x = Normal\ (0, \sigma_x^2) \tag{45}$$

$$y = Normal\ (0, \sigma_x^2) \tag{46}$$

$$\sigma_x\ = \left[\frac{\Gamma(1+\alpha)\sin(\frac{\alpha\pi}{2})}{\Gamma\left(\frac{(1+\alpha)}{2}\right)\alpha\, 2^{\frac{(\alpha-1)}{2}}}\right]^{1/\alpha} and\ \sigma_x\ = 1 \text{ dan } \alpha = 1.5 \tag{47}$$

Where Γ is Gamma function. Mantegna presented a precise and quick algorithm to produce stable Lévy flight processes for the index distribution's absolute values (α) [0.3 and 1.99]. x and y are two normally distributed variables with standard deviations σ_x and σ_y. α is the distribution index and controls the scale properties of the process while γ selects the scale units.

2.3. DC Motor

The DC motor has two control modes and all the characteristics of a single control system. The field current in the first mode, the armature control mode, is constant. However, it is known as a field control model

and has a fixed armature current. The features of a DC motor, such as resistance, inductance, and reverse electromotive force voltage, are depicted in Figure 1. Armature resistance and inductance are represented by R_a and L_a, respectively. The electromotive force in reverse is e_b.

$$V_a(s) = (R_a + L_a.s).I_a(s) + e_b(s) \tag{48}$$

$$e_b(s) = K_b\omega(s) \tag{49}$$

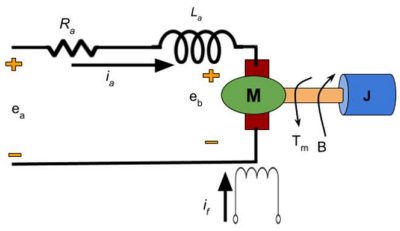

Figure 1. Illustration DC motor circuit

Table 1. DC motor parameters

Parameter	Value
K_b	0.05 V.s
L_a	2 H
R_a	0.4 Ω
J	0.0004 kg.m2
B	0.0022 N · m · s⁄rad
K_M	0.015 N · m⁄A

2.4. Proposed Levy Tornado Optimizer with Coriolis Force (LTOC)

The stability of the exploration and exploitation regions. Finding a new equilibrium between improved exploration and exploitation is the aim of this work.Tthis study suggests enhancements to the TOC method by incorporating the Levy Flight approach. Eq. 44 is put into Eq. 35 to become Eq. 50. The proposed method of algorithm can be seen in algorithm 1

$$\overrightarrow{y_{t_i}^t} = \overrightarrow{y_{t_i}^t} + 2 \times \alpha \times \left(\overrightarrow{y_{t_i}^t} - \overrightarrow{y_{o_\zeta}^t}\right) + Levy(\alpha) \tag{50}$$

Algorithma 1. A pseudo code of LTOC

1. Definision and initialize the parameter setting of TOC
2. $t \leftarrow$ Iteration counter
3. $T \leftarrow$ Maximum number of iterations
4. $n \leftarrow$ Population size
5. $n_w \leftarrow$ Number of windstorms
6. $n_t \leftarrow$ Number of thunderstorms
7. Create a random initial population using Eq. 18.
8. Evaluate the position of the initial population using Eq. 26.
9. **While** $(t \leq T)$ **do**
10. Update the adaptive parameters using the resprective formulas
11. **for** i=1 to n_w **do**
12. **if** $(rand \geq 0.5)$ **then**
13. $\vec{v}_i^{t+1} = \eta\left(\mu\vec{v}_i^t - c\frac{(f\times R_1}{2} + \sqrt{CF_l}\right)$
14. **else**
15. $\vec{v}_i^{t+1} = \eta\left(\mu\vec{v}_i^t - c\frac{(f\times R_1}{2} + \sqrt{CF_r}\right)$
16. **end if**
17. **end for**
18. **for** i=1 to n_w **do**
19. $\vec{y}_{w_i}^{t+1} = \vec{y}_{w_i}^t + 2 \times \alpha \times \left(\vec{y}_{w_i}^t - rand_w\right)\vec{v}_i^{t+1}$
20. **end for**
21. Investigate and update the feasibility of windstroms' positions
22. **for** i=1 to n_t **do**
23. **for** j=1 to n_{w_i} **do**
24. $\vec{y}_{w_{j+\Sigma_1^{nw}k}}^t = \vec{y}_{w_{j+\Sigma_1^{nw}k}}^t + 2 \times rand \times \left(\vec{y}_{t_i}^t - \vec{y}_{w_{j+\Sigma_1^{nw}k}}^t\right) + 2 \times rand \times \left(\vec{y}_{o_i}^t - \vec{y}_{w_{j+\Sigma_1^{nw}k}}^t\right)$
25. **end for**
26. **end for**
27. Investigate and update the feasibility of windstroms' positions
28. **for** i=1 to n_t **do**

Algorithma 1. A pseudo code of LTOC

$\overrightarrow{y_{t_\iota}^t} = \overrightarrow{y_{t_\iota}^t} + 2 \times \alpha \times \left(\overrightarrow{y_{t_\iota}^t} - \overrightarrow{y_{o_\zeta}^t}\right) + Levy(\alpha)$ eq. (50)
end for
Investigate and update the feasibility of windstroms' positions
for i=1 to n_w **do**
  if $\left\|\vec{y}_{w_i}^t - \vec{y}_{o_i}^t\right\| < v$ **then**
    $\vec{y}_{w_i}^{t+1} = \vec{y}_{w_i}^t - (2 \times \alpha_y \times (rand \times (l-u) - l)) \times \delta_2$
  end if
end for
for i=1 to n_t **do**
  if $\left\|\vec{y}_{w_i}^t - \vec{y}_{t_i}^t\right\| < v$ **then**
    For j=1 to n_{w_i} **do**
      $\vec{y}_{w_{j+\Sigma_{i=1}^{n_w} k}}^{t+1} = \vec{y}_{w_{j+\Sigma_{i=1}^{n_w} k}}^t - (2 \times \alpha_y \times (rand \times (l-u) - l)) \times \delta_2$
    end for
  end if
end for
$t = t + 1$
Retain thre beadt solutions
end while

3. RESULTS AND DISCUSSION

3.1. Convergence Curve Profile

The outcomes of the TOC strategy and the suggested LTOC methodology are contrasted. This study uses benchmark functions to evaluate the effectiveness of LTOC. The first step is to assess the 23 CEC2017 benchmark functions. The definition of functions F1 through F7 is unimodal. Multimodality is indicated by functions F8 through F13. Fixed-dimensional multimodal functions represented by mathematical equations are denoted as F14–F23. MATLAB/Simulink software was used to run the simulations. The comparison of benchmark function outcomes using the LTOC approach is shown in Figure 2. Benchmarking in the context of metaheuristics refers to the process of evaluating and comparing the performance of metaheuristic algorithms using standardized test problems (benchmark problems) to assess their effectiveness, reliability, and efficiency. Its main benefits are Measuring metrics such as convergence speed, solution accuracy, stability, and the ability to avoid local optima. Benchmarking on metaheuristics is a critical tool to Ensure algorithms are reliable in a variety of scenarios, Encourage the development of new methods through systematic evaluation and provide a scientific basis for selecting algorithms according to practical needs. With benchmarking, researchers and practitioners can avoid subjective bias and focus on measurable improvements in solution quality.

In Figure 2 (a)-(g), which is a unimodal function, the LTOC method has better capabilities than the TOC method. A unimodal function is a mathematical function that has one global optimum (minimum or maximum) and does not have other local optimums. In the context of optimization, unimodal functions are used to test the ability of an algorithm to find the best solution without getting stuck in a local optimum [48]-[51].

In Figure 2 (h)-(m) which is a multimodal function, LTOC has a better convergence curve than the TOC method. A multimodal function is a mathematical function that has many local optima (minimums or maxima) in addition to one or more global optima. This function challenges optimization algorithms because of the presence of local optimum "traps" that can hinder the search for the best solution. Multimodal functions are commonly used in metaheuristic benchmarking to test the algorithm's ability to navigate complex search spaces [52]-[55].

In Figure 2 (n)-(w) which is a Fixed-dimensional multimodal function, the curve of LTOC has the same convergence as the TOC method. Fixed-dimensional Multimodal Function is a multimodal optimization function (having many local optima and one or more global optima) defined in a fixed dimension (a constant number of variables/inputs, such as 2D, 5D, or 10D). Unlike the scalable multimodal function (which can be tested in different dimensions), this function is specifically designed for evaluating algorithms in a search space with a fixed complexity. This function is commonly used in metaheuristic benchmarking to test the ability of algorithms to navigate complex landscapes without being affected by changes in dimension [56]-[59].

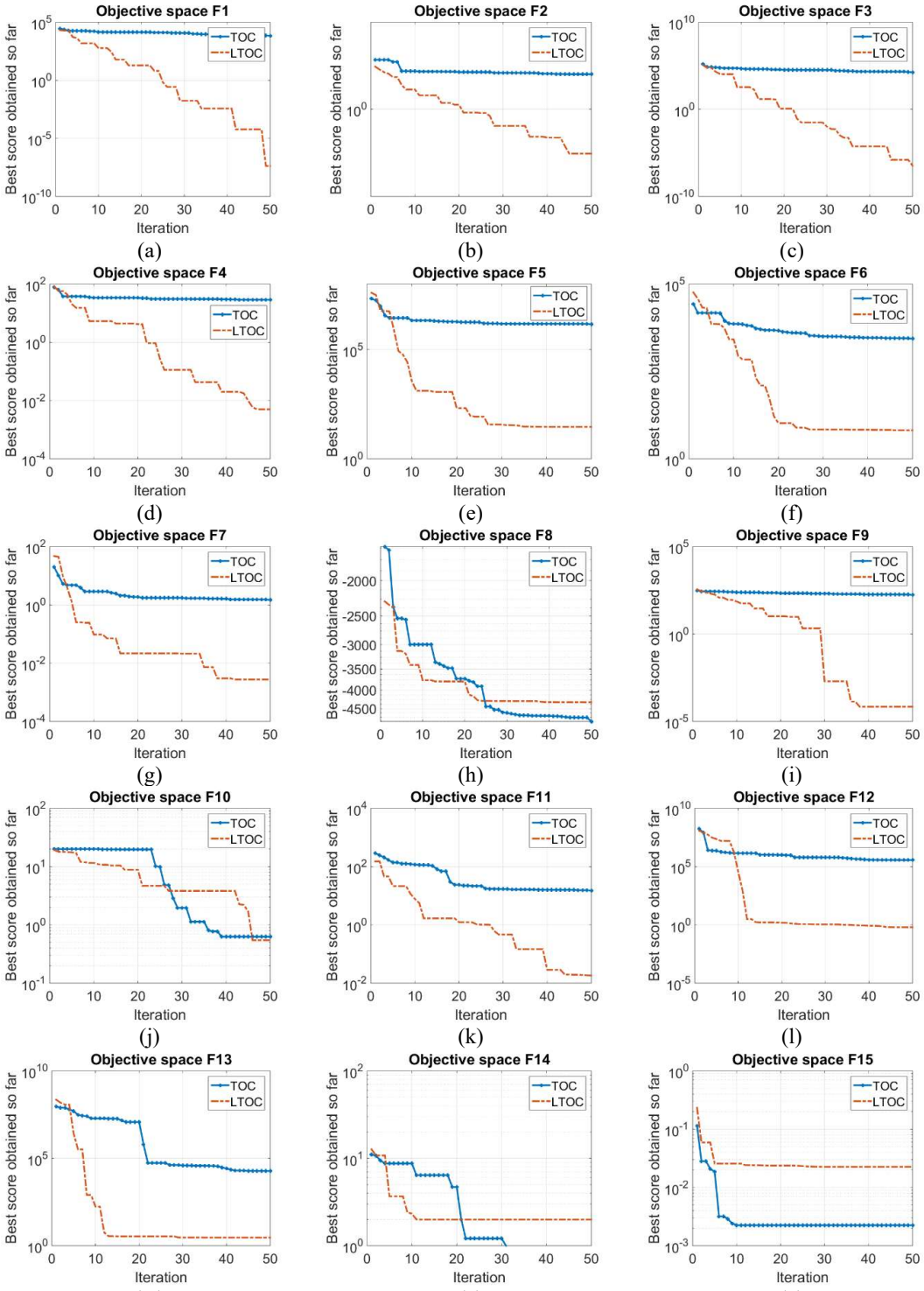

Figure 2. Convergence curve of benchmark function (a) F1, (b) F2, (c) F3, (d) F4, (e) F5, (f) F6, (g) F7, (h) F8, (i) F9, (j) F10, (k) F11, (l) F12, (m) F13, (n) F14, (o) F15

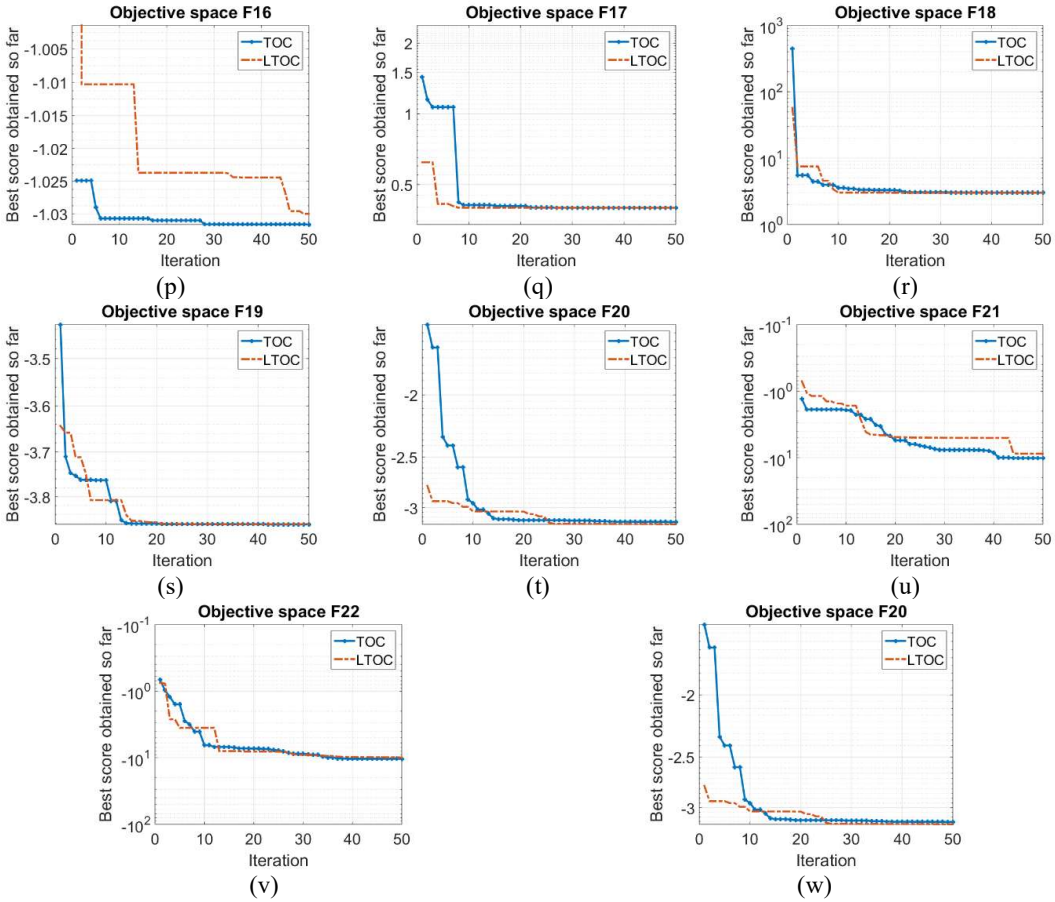

Figure 2. Convergence curve of benchmark function; (p) F16, (q) F17, (r) F18, (s) F19, (t) F20, (u) F21, (v) F22, (w) F23 (continue)

3.2. Applied To DC Motor

The DC motor's initial reference is 1 pu from the first to the fourth seconds. The DC motor reference value rises to 1.5 pu in the fourth second. This value is valid through the eighth second. The reference value then decreases to 0.5 pu at the eighth second. Figure 3 displays the controller's DC motor speed reaction output. Table 2 shows the controller's transient response analysis. The ITAE value of LTOC-PID for this method, which is 0.5380, is the lowest value among the other ways, according to the comparison of the overshoot values shown in Table 2. With an ITSE of 0.7161, the LTOC-PID approach has the lowest ITSE.

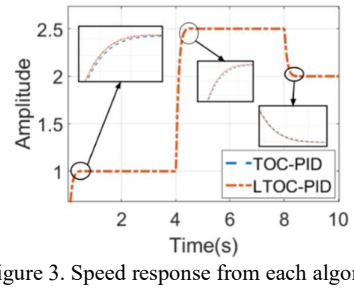

Figure 3. Speed response from each algorithm

Table 2. Result of responcse DC Motor

Controller	Time 0-4 s		Time 4-8 s		Time 8-10 s		ITSE	ITAE
	Overshoot	Risetime	Overshoot	Risetime	Undershoot	Risetime		
TOC-PID	0.1019	0.195	0.0645	4.195	0	8.19236	0.7162	0.5382
LTOC-PID	0.0779	0.194	0.468	4.194	0	8.19231	0.7161	0.5380

4. CONCLUSION

This article presents DC motor control utilizing the Modified Tornado optimizer-based Coriolis force (TOC) approach. The Tornado Optimizer-Based Coriolis Force Algorithm, a metaheuristic that uses tornado dynamics and the Coriolis force's effect to tackle challenging optimization issues, is the model for the TOC method. This study suggests improving the TOC method by incorporating the Levy Flight approach. The LTOC approach has the potential to expand exploration and exploitation based on the outcomes of experiments using optimal functions. In the meantime, the best overshoot response value is obtained when the LTOC approach is used as a DC motor controller. The LTOC approach outperforms the TOC method by 0.014% and 0.037%, respectively, in terms of ITSE and ITAE values.

REFERENCES

[1] M. Müller, M. Pfeifer, D. Holtz, & K. Müller, "Comparison of Green Ammonia and Green Hydrogen Pathways in Terms of Energy Efficiency," *Fuel*, vol. 357, pp. 129843, 2024. https://doi.org/10.1016/j.fuel.2023.129843.

[2] Y. Zhou and J. Liu, "Advances in Emerging Digital Technologies for Energy Efficiency and Energy Integration in Smart Cities," *Energy and Buildings*, vol. 315, pp. 114289, 2024. https://doi.org/10.1016/j.enbuild.2024.114289.

[3] A. Shahzad, F. Ahmad, S. Atiq, M. Saleem, O. Munir, M. Khan et al., "Harnessing the Potential of MOF-Derived Metal Oxide Composites to Optimize Energy Efficiency in Batteries and Supercapacitors," *Journal of Energy Storage*, vol. 87, pp. 111447, 2024. https://doi.org/10.1016/j.est.2024.111447.

[4] H. Qamar, G. Xiaoqiang, E. Ghith, & M. Tlija, "A Novel Approach to Energy Management with Power Quality Enhancement in Hydrogen Based Microgrids through Numerical Simulation," *Applied Sciences*, vol. 14, no. 17, pp. 7607, 2024. https://doi.org/10.3390/app14177607.

[5] Y. Teklehaimanot, F. Akingbade, B. Ubochi, & T. Ale, "A Review and Comparative Analysis of Maximum Power Point Tracking Control Algorithms for Wind Energy Conversion Systems," *International Journal of Dynamics and Control*, vol. 12, no. 9, pp. 3494-3516, 2024. https://doi.org/10.1007/s40435-024-01434-3.

[6] W. Ru, L. Zhang, D. Liu, N. Sun, M. Li, M. Faiz et al., "New Approach for Regional Water-Energy-Food Nexus Security Assessment: Enhancing the Random Forest Model with the Aquila Optimizer Algorithm," *Agricultural Water Management*, vol. 301, pp. 108946, 2024. https://doi.org/10.1016/j.agwat.2024.108946.

[7] A. Anh, P. Duc, & L. Huan, "Position Control to Expand the Headlights Angle of a Car by DC Motor Drive System using PSO Algorithm for Speed Loop," *Bulletin of Electrical Engineering and Informatics*, vol. 14, no. 2, pp. 874-882, 2025. https://doi.org/10.11591/eei.v14i2.8612.

[8] E. Natsheh, "Enhancing Field-Controlled DC Motors with Artificial Intelligence-Infused Fuzzy Logic Controller," *Journal of Applied Data Sciences*, vol. 6, no. 1, pp. 455-469, 2024. https://doi.org/10.47738/jads.v6i1.508.

[9] C. Eang and S. Lee, "Predictive Maintenance and Fault Detection for Motor Drive Control Systems in Industrial Robots Using CNN-RNN-Based Observers," *Sensors*, vol. 25, no. 1, pp. 25, 2024. https://doi.org/10.3390/s25010025.

[10] C. Yuan, X. Lyu, & S. Mao, "Optimization Design of Brushless DC Motor Based on Improved JAYA Algorithm," *Scientific Reports*, vol. 14, no. 1, pp. 5427, 2024. https://doi.org/10.1038/s41598-024-54582-z.

[11] K. Rambabu, S. Dubey, B. Reddy, M. Ezhilvendan, P. Prakash, P. Vamshi et al., "Automated Canine Food Vending Machine Using Yolo V5And Arduino," *2024 10th International Conference on Communication and Signal Processing (ICCSP)*, pp. 411-416, 2024. https://doi.org/10.1109/iccsp60870.2024.10543470.

[12] M. Jabari, S. Ekinci, D. İzci, M. Bajaj, & Є. Зайцев, "Efficient DC Motor Speed Control Using a Novel Multi-Stage FOPD(1 + PI) Controller Optimized by The Pelican Optimization Algorithm," *Scientific Reports*, vol. 14, no. 1, 2024. https://doi.org/10.1038/s41598-024-73409-5.

[13] D. Munciño, E. Damian-Ramírez, M. Cruz-Fernández, L. Montoya-Santiyanes, & J. Rodríguez-Reséndiz, "Metaheuristic and Heuristic Algorithms-Based Identification Parameters of a Direct Current Motor," *Algorithms*, vol. 17, no. 5, pp. 209, 2024. https://doi.org/10.3390/a17050209.

[14] T. Nizami, S. Gangula, R. Udumula, A. Chakravarty, F. Ahmad, & A. Hosseinpour, "Nonlinear Adaptive Neural Control of Power Converter-Driven DC Motor System: Design and Experimental Validation," *Engineering Reports*, vol. 7, no. 1, 2024. https://doi.org/10.1002/eng2.13025.

[15] A. Güven, O. MENGİ, M. Elseify, & S. Kamel, "Comprehensive Optimization of PID Controller Parameters for DC Motor Speed Management Using a Modified Jellyfish Search Algorithm," *Optimal Control Applications and Methods*, 2024. https://doi.org/10.1002/oca.3218.

[16] F. Zhao, T. Liu, Y. Ju, & H. Li, "Large Disturbance Stability Analysis Method for DC Microgrid with Virtual DC Motor Control," *IET Renewable Power Generation*, vol. 18, no. S1, pp. 4689-4706, 2024. https://doi.org/10.1049/rpg2.13179.

[17] D. Wubu, A. Salau, & G. Alitasb, "Particle Swarm Optimization Algorithm Based Fuzzy PID Controller Design for Speed Tracking Control of Separately Excited DC Motor," *Advanced Control for Applications*, vol. 6, no. 4, 2024. https://doi.org/10.1002/adc2.237.

[18] J. Zheng, X. Wang, X. Huang, Y. Shi, X. Zhang, Y. Wang et al., "Adaptive Control System of Header for Cabbage Combine Harvester Based on IPSO-Fuzzy PID Controller," *Computers and Electronics in Agriculture*, vol. 232, pp. 110044, 2025. https://doi.org/10.1016/j.compag.2025.110044.

[19] S. Saat, M. Ahmad, & M. Ghazali, "Data-Driven Brain Emotional Learning-based Intelligent Controller-PID Control of MIMO Systems based on a Modified Safe Experimentation Dynamics Algorithm," *International Journal of Cognitive Computing in Engineering*, vol. 6, pp. 74-99, 2025. https://doi.org/10.1016/j.ijcce.2024.11.005.

[20] B. Durusoy, N. Kaya, O. Okan, R. Budakoğlu, B. Akinoglu, & R. Turan, "Suppression of The Shunting-type Potential Induced Degradation (PID-S) Through Ion Exchange on Soda Lime Silicate Glasses," *Solar Energy Materials and Solar Cells*, vol. 283, pp. 113474, 2025. https://doi.org/10.1016/j.solmat.2025.113474.

[21] G. Chen, Y. Liang, Z. Jiang, S. Li, H. Li, & Z. Xu, "Fractional-Order PID-Based Search Algorithms: A Math-Inspired Meta-Heuristic Technique with Historical Information Consideration," *Advanced Engineering Informatics*, vol. 65, pp. 103088, 2025. https://doi.org/10.1016/j.aei.2024.103088.

[22] X. Song, Z. Fan, S. Lu, & W. Sai, "PID Dynamic Sliding Mode Fault-Tolerant Control with Time-Delay Estimation for Liquid-Filled Spacecraft with Large-Amplitude Sloshing," *Journal of Aerospace Engineering*, vol. 38, no. 3, p. 4025003, 2025. https://doi.org/10.1061/jaeeez.aseng-5777.

[23] A. Sánchez and F. Pérez-Pinal, "Fractional-Order PI/PD and PID Controllers in Power Electronics: The Step-Down Converter Case," *Integration*, vol. 102, pp. 102360, 2025. https://doi.org/10.1016/j.vlsi.2025.102360.

[24] A. Şahin and M. Ayas, "Fine-Tuned Design of the PIDFFD2F Control Strategy for the Functional Electrical Stimulation System using Dandelion Optimizer," *Biomedical Signal Processing and Control*, vol. 103, pp. 107350, 2025. https://doi.org/10.1016/j.bspc.2024.107350.

[25] M. El-Dabah and A. Agwa, "Identification of Transformer Parameters using Dandelion Algorithm," *Applied System Innovation*, vol. 7, no. 5, pp. 75, 2024. https://doi.org/10.3390/asi7050075.

[26] S. Chandini and A. Rajendra, "Hybridized Grasshopper Optimization and Cuckoo Search Algorithm for the Classification of Malware," *Bulletin of Electrical Engineering and Informatics*, vol. 13, no. 5, pp. 3616-3627, 2024. https://doi.org/10.11591/eei.v13i5.7548.

[27] 蒋杰伟, 金库, 朱少民, **刘尚辉**, and **巩稼民**, "基于 CNN-LSTM 和海马优化算法的二阶拉曼光纤放大器设计方案," *J. Optoelectron. Laser*, vol. 35, no. 10, pp. 1009–1017, 2024. http://doi.org/10.16136/j.joel.2024.10.0090.

[28] Z. Zhang, X. Wang, & Y. Yue, "Heuristic Optimization Algorithm of Black-Winged Kite Fused with Osprey and Its Engineering Application," *Biomimetics*, vol. 9, no. 10, pp. 595, 2024. https://doi.org/10.3390/biomimetics9100595.

[29] M. Jabari, D. İzci, S. Ekinci, M. Bajaj, V. Blažek, & L. Prokop, "A Novel Artificial Intelligence Based Multistage Controller for Load Frequency Control in Power Systems," *Scientific Reports*, vol. 14, no. 1, 2024. https://doi.org/10.1038/s41598-024-81382-2.

[30] H. Fakhouri, M. Alkhalaileh, F. Hamad, N. Sirhan, & S. Fakhouri, "Hybrid Arctic Puffin Algorithm for Solving Design Optimization Problems," *Algorithms*, vol. 17, no. 12, pp. 589, 2024. https://doi.org/10.3390/a17120589.

[31] I. Hattabi, A. Kheldoun, R. Bradai, S. Khettab, A. Sabo, Y. Belkhier et al., "Enhanced Power System Stabilizer Tuning Using Marine Predator Algorithm with Comparative Analysis and Real Time Validation," Sc*ientific Reports*, vol. 14, no. 1, 2024. https://doi.org/10.1038/s41598-024-80154-2.

[32] Y. Wang, H. Song, J. Wang, Y. Song, Y. Qi, & X. Ma, "GOG-MBSHO: Multi-Strategy Fusion Binary Sea-Horse Optimizer with Gaussian Transfer Function for Feature Selection of Cancer Gene Expression Data," *Artificial Intelligence Review*, vol. 57, no. 12, 2024. https://doi.org/10.1007/s10462-024-10954-5.

[33] S. Gopi and P. Mohapatra, "Chaotic Aquila Optimization Algorithm for Solving Global Optimization and Engineering Problems," *Alexandria Engineering Journal*, vol. 108, pp. 135-157, 2024. https://doi.org/10.1016/j.aej.2024.07.058.

[34] B. Abed-alguni, B. Alzboun, & N. Alawad, "BOC-PDO: An Intrusion Detection Model Using Binary Opposition Cellular Prairie Dog Optimization Algorithm," *Cluster Computing*, vol. 27, no. 10, pp. 14417-14449, 2024. https://doi.org/10.1007/s10586-024-04674-2.

[35] M. Khattap, M. Elaziz, H. Hassan, A. Elgarayhi, & M. Sallah, "AI-Based Model for Automatic Identification of Multiple Sclerosis Based On Enhanced Sea-Horse Optimizer and MRI Scans," *Scientific Reports*, vol. 14, no. 1, 2024. https://doi.org/10.1038/s41598-024-61876-9.

[36] S. Wang, L. Cao, Y. Chen, C. Chen, Y. Yue, & W. Zhu, "Gorilla Optimization Algorithm Combining Sine Cosine and Cauchy Variations and Its Engineering Applications," *Scientific Reports*, vol. 14, no. 1, 2024. https://doi.org/10.1038/s41598-024-58431-x.

[37] N. Li and Y. Shi, "Adaptive Endocrine PID Control for Active Suspension Based on Reinforcement Learning," *Proceedings of the Institution of Mechanical Engineers, Part D: Journal of Automobile Engineering*, 2024. https://doi.org/10.1177/09544070241262354.

[38] M. Jabari, D. İzci, S. Ekinci, M. Bajaj, & Є. Зайцев, "Performance Analysis of DC-DC Buck Converter with Innovative Multi-Stage PIDN(1+PD) Controller using GEO Algorithm," *Scientific Reports*, vol. 14, no. 1, 2024. https://doi.org/10.1038/s41598-024-77395-6.

[39] C. Hu, F. Wu, & H. Zou, "New PID Parameter Tuning Based on Improved Dung Beetle Optimization Algorithm," *The Canadian Journal of Chemical Engineering*, vol. 102, no. 12, pp. 4297-4316, 2024. https://doi.org/10.1002/cjce.25343.

[40] C. Ersalı and B. Hekimoğlu, "A Novel Opposition-Based Hybrid Cooperation Search Algorithm with Nelder–Mead for Tuning of FOPID-Controlled Buck Converter," *Transactions of the Institute of Measurement and Control*, vol. 46, no. 10, pp. 1924-1942, 2024. https://doi.org/10.1177/01423312231214593.

[41] Y. Danayiyen, K. Dincer, & Y. Nuhoğlu, "A Novel Fractional Order Proportional Integral-Fractional Order Proportional Derivative Controller Design Based on Symbiotic Organisms Search Algorithm for Speed Control of a Direct Current Motor," *Electrica*, vol. 24, no. 2, pp. 327-335, 2024. https://doi.org/10.5152/electrica.2024.23076.

[42] Y. K. Kirange and P. Nema, "Optimization of PID Controller Parameters for An SMIB System using a Hybrid Butterfly Particle Swarm Optimization Approach," *International Journal of Advanced Technology and Engineering Exploration*, vol. 11, no. 113, 2024. https://doi.org/10.19101/ijatee.2023.10102286.

[43] D. İzci and S. Ekinci, "Fractional Order Controller Design via Gazelle Optimizer for Efficient Speed Regulation of Micromotors," *E-Prime - Advances in Electrical Engineering, Electronics and Energy*, vol. 6, pp. 100295, 2023. https://doi.org/10.1016/j.prime.2023.100295.

[44] I. Altawil, M. Momani, M. Tahat, R. Athamneh, M. Al-Saadi, & Z. Albataineh, "Optimization of Fractional Order PI Controller to Regulate Grid Voltage Connected Photovoltaic System Based on Slap Swarm Algorithm," *International Journal of Power Electronics and Drive Systems (IJPEDS)*, vol. 14, no. 2, pp. 1184, 2023. https://doi.org/10.11591/ijpeds.v14.i2.pp1184-1200.

[45] A. Ghany and M. Shamseldin, "Fuzzy Type Two Self-Tuning Technique of Single Neuron PID Controller for Brushless DC Motor Based on a COVID-19 Optimization," *International Journal of Power Electronics and Drive Systems (IJPEDS)*, vol. 14, no. 1, pp. 562, 2023. https://doi.org/10.11591/ijpeds.v14.i1.pp562-576.

[46] L. Fong, M. Islam, & M. Ahmad, "Optimized PID Controller of DC-DC Buck Converter based on Archimedes Optimization Algorithm," *International Journal of Robotics and Control Systems*, vol. 3, no. 4, pp. 658-672, 2023. https://doi.org/10.31763/ijrcs.v3i4.1113.

[47] M. Braik, H. Al-Hiary, H. Al-Zoubi, A. Hammouri, M. Al-Betar, & M. Awadallah, "Tornado Optimizer with Coriolis Force: A Novel Bio-Inspired Meta-Heuristic Algorithm for Solving Engineering Problems," *Artificial Intelligence Review*, vol. 58, no. 4, 2025. https://doi.org/10.1007/s10462-025-11118-9.

[48] S. Omari, K. Kaabneh, I. Abu-Falahah, K. Eguchi, S. Gochhait, I. Leonova et al., "Dollmaker Optimization Algorithm: A Novel Human-Inspired Optimizer for Solving Optimization Problems," *International Journal of Intelligent Engineering and Systems*, vol. 17, no. 3, pp. 816-828, 2024. https://doi.org/10.22266/ijies2024.0630.63.

[49] H. Yu, H. Liu, S. Zhang, J. Zhang, & Z. Han, "Prediction of Gas–Solid Erosion Wear of Bionic Surfaces Based on Machine Learning and Unimodal Intelligent Optimization Algorithm," *Engineering Failure Analysis*, vol. 163, pp. 108453, 2024. https://doi.org/10.1016/j.engfailanal.2024.108453.

[50] S. Javed, K. Zafar, & I. Younas, "Kids Learning Optimizer: Social Evolution and Cognitive Learning-Based Optimization Algorithm," *Neural Computing and Applications*, vol. 36, no. 28, pp. 17417-17465, 2024. https://doi.org/10.1007/s00521-024-10009-4.

[51] I. Falahah, O. Al-Baik, S. Alomari, G. Bektemyssova, S. Gochhait, I. Leonova et al., "Frilled Lizard Optimization: A Novel Bio-Inspired Optimizer for Solving Engineering Applications," *Computers, Materials & Continua*, vol. 79, no. 3, pp. 3631-3678, 2024. https://doi.org/10.32604/cmc.2024.053189.

[52] Z. Liao, Q. Pang, & Q. Gu, "Differential Evolution Based on Strategy Adaptation and Deep Reinforcement Learning for Multimodal Optimization Problems," *Swarm and Evolutionary Computation*, vol. 87, pp. 101568, 2024. https://doi.org/10.1016/j.swevo.2024.101568.

[53] S. Cheng, X. Wang, M. Zhang, X. Lei, H. Lü, & Y. Shi, "Solving Multimodal Optimization Problems by a Knowledge-Driven Brain Storm Optimization Algorithm," *Applied Soft Computing*, vol. 150, pp. 111105, 2024. https://doi.org/10.1016/j.asoc.2023.111105.

[54] J. Liang, H. Lin, C. Yue, P. Suganthan, & Y. Wang, "Multiobjective Differential Evolution for Higher-Dimensional Multimodal Multiobjective Optimization," *IEEE/CAA Journal of Automatica Sinica*, vol. 11, no. 6, pp. 1458-1475, 2024. https://doi.org/10.1109/jas.2024.124377.

[55] S. Suriyaraj, D. Ganapathy, & D. Shanmugamprema, "Prehabilitation Strategies: Enhancing Surgical Resilience with a Focus on Nutritional Optimization and Multimodal Interventions," *Advances in Nutrition*, vol. 16, no. 4, pp. 100392, 2025. https://doi.org/10.1016/j.advnut.2025.100392.

[56] H. Özmen, S. Ekinci, & D. İzci, "Boosted Arithmetic Optimization Algorithm with Elite Opposition-Based Pattern Search Mechanism and Its Promise to Design Microstrip Patch Antenna for WLAN and WiMAX," *International Journal of Modelling and Simulation*, vol. 45, no. 1, pp. 264-279, 2023. https://doi.org/10.1080/02286203.2023.2196736.

[57] S. Alomari, K. Kaabneh, I.A. Falahah, S. Gochhait et al., "Carpet Weaver Optimization: A Novel Simple and Effective Human-Inspired Metaheuristic Algorithm," *International Journal of Intelligent Engineering and Systems*, vol. 17, no. 4, pp. 230-242, 2024. https://doi.org/10.22266/ijies2024.0831.18.

[58] S. Ekinci, D. İzci, & A. Hussien, "Comparative Analysis of The Hybrid Gazelle-Nelder–Mead Algorithm for Parameter Extraction and Optimization of Solar Photovoltaic Systems," *IET Renewable Power Generation*, vol. 18, no. 6, pp. 959-978, 2024. https://doi.org/10.1049/rpg2.12974.

[59] H. Fakhouri, F. Awaysheh, S. Alawadi, M. Alkhalaileh, & F. Hamad, "Four Vector Intelligent Metaheuristic for Data Optimization," *Computing*, vol. 106, no. 7, pp. 2321-2359, 2024. https://doi.org/10.1007/s00607-024-01287-w.

BIOGRAPHIES OF AUTHORS

Diego Oliva is an Associate Professor at the University of Guadalajara in Mexico. He has the distinction of National Researcher Rank 2 by the Mexican Council of Science and Technology. Currently, he is a Senior member of the IEEE. His research interests include evolutionary and swarm algorithms, hybridization of evolutionary and swarm algorithms, computational intelligence, and image processing. He can be contacted at email: diego.oliva@cucei.udg.mx.

Farhad Soleimanian Gharehchopogh received his B.S. in computer engineering from Shabestar Branch, Islamic Azad University, West Azerbaijan, Iran, in 2002, the M.S. in computer engineering from Cukurova University, Adana, Turkey, in 2011 and the Ph.D. degree in computer engineering from Hacettepe University, Ankara, Turkey in 2015. He has been an academic staff member in computer engineering at Urmia Branch, Islamic Azad University, Urmia, IRAN, from 2015 to now. He can be contacted at email: bonab.farhad@gmail.com.

Vugar Hacimahmud Abdullayev is Professor of the "Computer Engineering" Department at the Azerbaijan State Oil and Industry University, Baku, Azerbaijan. His research is related to the study of cyber-physical systems, IoT, big data, smart cities and information technologies. ORCID: 0000-0002-3348-2267.

Widi Aribowo is a lecturer in the Department of Electrical Engineering, Universitas Negeri Surabaya, Indonesia. He is received the BSc from the Sepuluh Nopember Institute of Technology (ITS) in Power Engineering, Surabaya in 2005. He is received the M.Eng from the Sepuluh Nopember Institute of Technology (ITS) in Power Engineering, Surabaya in 2009. He is mainly research in the power system and control. He can be contacted at email: widiaribowo@unesa.ac.id.

Asmunin is a lecturer in the Department of Informatics, Universitas Negeri Surabaya, Indonesia. He is received the BSc from the Sepuluh Nopember Institute of Technology (ITS) in Informatics Engineering, Surabaya in 2005. He is received the M.Sc from the Sepuluh Nopember Institute of Technology (ITS) in Informatics Engineering, Surabaya in 2016. He is mainly research in the maching learning dan steganography. He can be contacted at email: asmunin@unesa.ac.id.

Andi Iwan Nurhidayat is a lecturer in the Department of Informatics, Universitas Negeri Surabaya, Indonesia. He is received the BSc from the Sepuluh Nopember Institute of Technology (ITS) in Informatics Engineering, Surabaya in 2005. He is received the M.Sc from the Sepuluh Nopember Institute of Technology (ITS) in Informatics Engineering, Surabaya in 2016. He is mainly research in the maching learning dan webometrics. He can be contacted at email: andyl34k5@unesa.ac.id.